Arab J Sci Eng (2016) 41:4775–4785
DOI 10.1007/s13369-016-2190-7

RESEARCH ARTICLE - CHEMICAL ENGINEERING

Synthesis of Bentonite–Carbon Nanotube Nanocomposite and Its Adsorption of Rhodamine Dye From Water

Mohammed Ibrahim Mohammed[1] · **Sitki Baytak**[2]

Received: 8 January 2016 / Accepted: 11 May 2016 / Published online: 28 May 2016

Abstract In this work, cheap and effective nanocomposite material has been synthesized by mixing natural bentonite (B) with 5 % multiwall carbon nanotubes followed by heat treatment to 650 °C in the inert atmosphere. It makes a potentially attractive adsorbent of rhodamine dye (RhB) from wastewater. The nanocomposite adsorbent (BCA) was characterized by X-ray diffraction, scanning electron microscopy and Fourier transform infrared spectroscopy. The effects of contact time, adsorbent dosage, initial dye concentration and pH on dye removal were investigated. The isotherm of dye adsorption was studied. The adsorption isotherm of dye onto B and BCA showed good fitting to Langmuir and Freundlich isotherm models. The maximum adsorption capacity (q_m) of B and BCA samples is 8.6 and 142.8 mg/g, respectively. Both bentonite and modified bentonite are capable of removing the RhB dye from water. In general, the nanocomposite sample BCA significantly enhances the removal of RhB dye from aqueous solution. In addition, the BCA could be used as an eco-friendly adsorbent to remove the dye from colored wastewater.

Keywords Adsorption · Nanocomposite BCA · Bentonite · Dye removal

List of Symbols

B	Raw bentonite
BCA	Bentonite carbon nanotubes (nanocomposite) adsorbent
RhB	Rhodamine dye
CNTs	Multiwall carbon nanotubes
FWHM	Full width at half maximum
D	The average crystallite size (nm)
λ	The wavelength of the X-ray radiation (nm)
K	The Scherrer constant ($k = 0.9$)
β	The half maximum line breadth
θ	The Bragg angle
m	Mass of adsorbent (g/L)
q	q (mg/g) is adsorption capacity or amount of adsorbate removed from aqueous solution at equilibrium
C_e	Concentration of the adsorbate at equilibrium in the solution (mg/L)
q_m	Maximum adsorption capacity (mg/g)
K_L	Langmuir constant (L/g)
K_F	Freundlich constant indicating the adsorption capacity of the adsorbent (mg/g)
n	Experimental constant indicative of the adsorption intensity of the adsorbent
C_0	The initial concentration of the dye (mg/L)
RL	Equilibrium parameter describing the type of Langmuir isotherm

1 Introduction

The textile industry is one of the main polluters in the world. The World Bank has estimated that almost 20 % of world industrial water pollution comes from the treatment

✉ Mohammed Ibrahim Mohammed
mohab1964@yahoo.com

[1] Chemical Engineering Department, University of Technology, Baghdad, Iraq

[2] Chemical Engineering Department, University of Suleyman Demirel, Isparta, Turkey

and dyeing of textiles. Dyes can be of many different structural varieties like acidic, basic, disperse, azo, anthraquinone based and metal complex dyes, among others. During the coloration process, a large percentage of the synthetic dye does not bind and is dropped into a waste stream [1]. Dyes are very stable and can only decompose at temperatures over 200 °C [2]. So, they are considered strongly hazardous and can cause harmful effects. For this reason, synthetic dyes often receive great attention from researchers in the textile wastewater treatment process. Various techniques have been used for organic dye removal from wastewater such as flocculation, an aerobic biological treatment, membrane separation, sonolysis, oxidation destruction via UV/ozone treatment and photocatalytic degradation biodegradation which have certain efficiency, but initial and operational costs are too high [3–6].

Among these methods, adsorption is considered an important method that is commonly used for removal of colorant in the industrial process [7,8]. Several adsorbents have been applied to dye removal, such as activated carbon [9], alumina [10], clay [11], bentonite [12,13], combined treatment of lime and alum [14], zeolite [15] and carbon nanotubes [16]. Although bentonite exhibits great potential for adsorption of dyes from aqueous solution, the adsorption capacity remains limited [17]. The modification of bentonite is therefore considered to be necessary for the enhancement of dye removal efficiency. Much work has been done to improve the adsorption of bentonite efficiency by acid activation and surface modification, particulary in recent years. Much less has been published on experiments to use the nanoparticles in bentonite modification. Carbon nanotube (CNTs), because of its high reactivity due to large surface area-to-volume ratio, has proven to possess great potential for removing many kinds of pollutants and dyes [18–24], but CNTs tend to aggregate and make the dispersion of water CNTs even more difficult because of their intrinsic hydrophobic nature [25]. Also, they make their dispersion a significant challenge in the host polymer matrix [26]. Moreover, chemical modification methods for bentonite and CNTs contaminate water environment because of using a high quantity of water for neutralization. Therefore, the aim of the present work is the synthesis of bentonite–carbon nanotube nanocomposite (BCA) adsorbent which possesses high adsorption capacity, high dispersibility in water and low cost of manufacturing.

The adsorption mechanism of rhodamine dye (RhB) was examined using the new modified bentonite nanocomposite. The effects of parameters such as dye concentration, contact time, the mass of adsorbent and pH of the solution on dye removal were investigated. Natural bentonite was tested as a reference.

2 Material and Methods

2.1 Chemicals

Bentonite (CaB) was obtained from the bed in the Al-Anbar region. It was supplied by Iraqi National Company for Geological Survey and Mining. The chemical composition of bentonite is given in Table 1.

Graphitized multiwall carbon nanotubes (CNTs) of 5 nm outer diameter and 30 μm in length were supplied by Soochow Hengqiu Technology Co., China. The specific surface area as determined by BET methods was 59 m^2/g for bentonite B and 166 m^2/g for CNTs.

The dye used in this work was Rhodamine RhB and is one of the commonly used in textile factories. RhB has a maximum absorption wavelength of 555 nm, molecular formula of $C_{28}H_{31}N_2O_3Cl$, molecular weight 479 and the following structure feature:

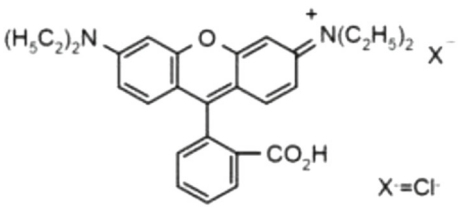

All other chemicals were of analytical grade and were purchased from Merck (Germany).

2.2 Characterization of Adsorbents

The composition and crystalline structure of both B and BCA samples were determined from XRD patterns using X'Pert Pro (Panalytical) diffractometer with Ni-filtered 1.54 Kα Cu radiation. FTIR spectra of the CNTs, B and BCA samples were recorded in the region of 4000–400 cm^{-1} on a Perkin-Elmer Spectrum BX automatic FTIR spectrometer at 4 cm^{-1} resolution. The surface morphology of B and BCA samples was obtained by scanning electron microscope (SEM). The concentration of RhB Dye in aqueous solution was measured by using UV–visible spectrophotometer (Cary 60, Agilent Technology, Germany).

Table 1 The chemical composition of bentonite

Chemical composition	SiO_2	Al_2O_3	Fe_2O_3	CaO	MgO	Na_2O	K_2O	L.O.I
Wt. (%)	56.77	15.67	5.03	4.48	3.42	1.11	0.60	12.49

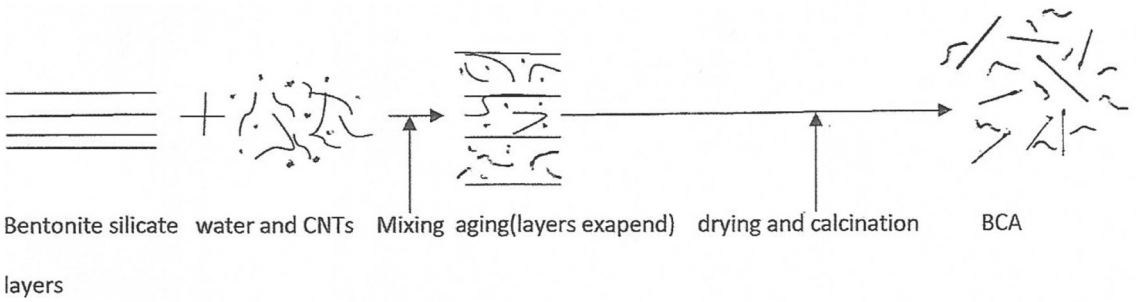

Fig. 1 BCA nanocomposite preparation process

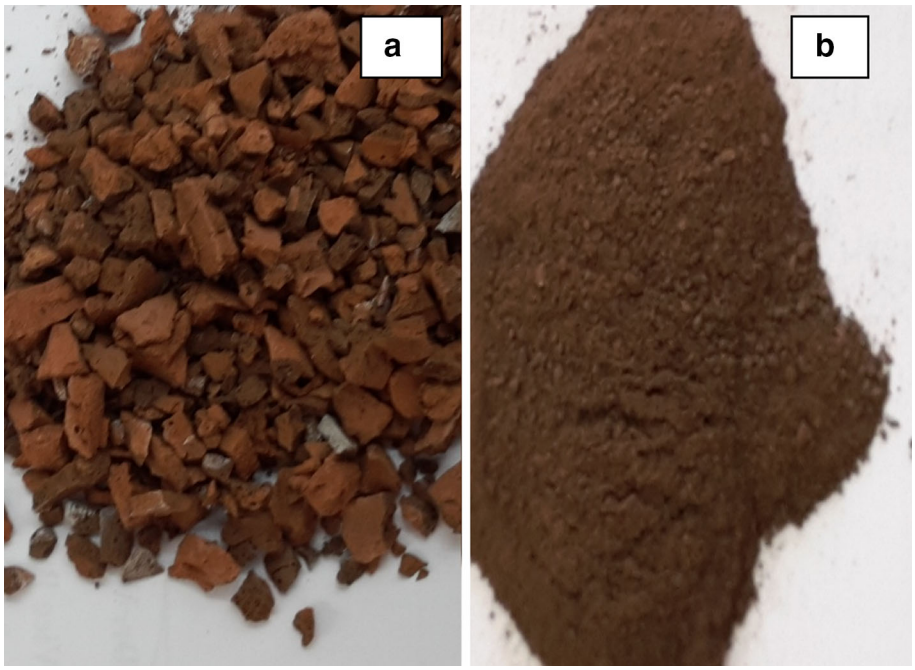

Fig. 2 BCA sample before grounding (**a**) and after grounding (**b**)

2.3 Preparation of Bentonite–CNTs Composite Adsorbent (BCA)

The preparation process of BCA adsorbent included 4 main steps: preparation of bentonite raw material, mixing with CNTs, aging, drying and calcination. Preparation scheme is presented in Fig. 1.

A sample of raw bentonite was washed several times with distilled water and dried in oven at a temperature of 80 °C for 24h. The dried bentonite was ground and sieved by 200-mesh sieve. The sample was labeled B and kept in a dry place.

The modified bentonite sample BCA was prepared by mixing 4.6 g (200 mesh) of dry sample B with 5 % (0.4 g) of multiwall carbon nanotubes using the mechanical mixer. Distilled water was added to the mixture with continuous stirring at room temperature. When the mixture became viscous, it was placed in a tight plastic container and aged for 72 h. After aging, the sample was taken out of the container, divided into small pieces and dried in an oven at 120 °C for 12 h. Then the sample was allowed to cool at room temperature. Calcination was performed at 650 °C using tubular furnace under nitrogen inert atmosphere for 1h. The resulting hard pieces were ground into sizes less than 200 meshes. The BCA composite sample before and after the grounding is shown in Fig. 2a, b.

The function of calcination at high temperature was to convert the structure of mixture into a primary phase of the ceramic structure.

2.4 Dye Adsorption Procedure

A stock solution of RhB was prepared by dissolving 1.0 g of dye powder in 1000 mL distilled water in an appropriate volumetric flask. The stock solution was diluted to prepare solution with different initial concentrations for adsorption experiments.

Sorption of dye was determined using a batch equilibrium method. Briefly, a known quantity of adsorbent was added in a 250-mL beaker containing 200 mL of RhB solu-

tion of known concentration and pH. The mixture was stirred by a magnetic stirrer at 250 rpm at room temperature. The resulting solution was separated by centrifuge at 4000 rpm for 10 min and filtered by a filter paper. The concentration (mg/L) of RhB dye in the filtrate was measured using UV–visible spectrophotometer (Gray-60) at 555 nm corresponding to maximum absorbency of RhB dye.

The equilibrium adsorption capacity was calculated using Eq. (1):

$$q = \frac{C_0 - C_f}{m} \times V \tag{1}$$

where q (mg/g) is adsorption capacity, m (g) is the mass of adsorbent, V (L) is the volume of solution, and C_0 and C_f (mg/L) are the dye solution concentration at initial and final conditions, respectively. The removal efficiency (R %) of the dye was calculated by the following relationship:

$$R\,(\%) = \frac{C_0 - C_f}{C_0} \times 100 \tag{2}$$

3 Result and Discussion

3.1 Characterization of Absorbent

The surface morphology of bentonite surface before and after CNTs loading was analyzed by a scanning electron microscope as shown in Fig. 3a, b respectively.

B samples reveal a dense sheet structure of original natural bentonite, as shown in Fig. 3b. The bentonite sheets were changed from a dense sheet to thin crystalline structure sheet decorated by CNTs as shown in Fig. 3b. CNTs seem to be either embedded within the structure of bentonite sheets or collected onto their surface. The formation of thin sheets

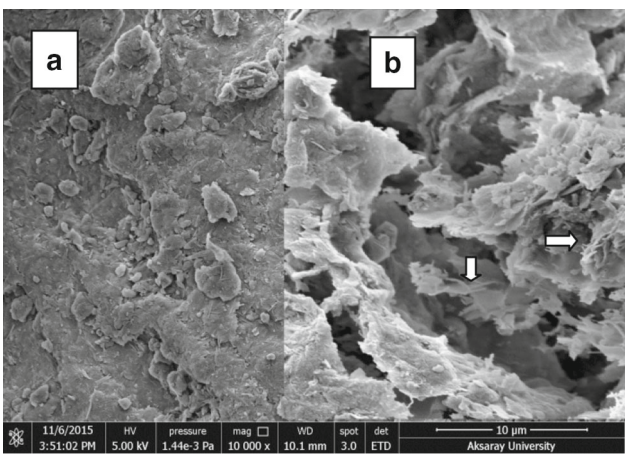

Fig. 3 Morphology of bentonite sample (**a**) and BCA sample (**b**)

can be attributed to the splitting of bentonite silicate layers in which the CNTs may have an influential role and to the reduction in bond of clay water as a result of the sample heating at 650 °C.

The XRD pattern of the bentonite sample (B) showed the presence of a montmorillonite phase with a small difference in crystallographic parameters of sample BCA, mainly due to the dehydration of bentonite during the heating up, as shown in Fig. 4a, b.

The XRD pattern of BCA sample shows a diminished kaolinite peak at $2\theta = 11.68°$, while the intensity of the bentonite peak at $2\theta = 19.83°$ is increased with a very slight change in d-spacing. The reflection peak at $2\theta = 26.69°$ due to the quartz line shows no change in intensities or in d-spacing, but increases in the full width at half maximum (FWHM) of the peak from 0.05° to 0.09° are observed. Based on XRD results, the crystallite size of quartz phase is calculated by the Scherrer equation:

$$D = \frac{K\lambda}{\beta \cos\theta} \tag{3}$$

where D is the average crystallite size (nm), λ the wavelength of the X-ray radiation (0.1540 nm), K the Scherrer constant ($k = 0.9$), β the half maximum line breadth (FWHM), and θ is the Bragg angle. The result shows a change in crystallite size of quartz phase from 139.79 nm of the B sample to 83.30 nm in BCA sample. The change in crystallite size may be attributed to the dehydration of interparticle water, adsorbed water and interlayer water [27]. It can be concluded that the formation of fine crystals is responsible for increasing surface area of modified sample. No CNTs peaks were detected either due to their quantity being less than the detection limit of XRD device or being overlapped by quartz peak at $2\theta = 26.69°$.

The FTIR spectra of the CNTs (C), bentonite sample (B) and the modified bentonite (BCA) sample are shown in Fig. 5. A spectrum of B reveals the band belonging to montmorillonite; the transmission band at 3628 cm^{-1} is due to the stretching vibration of structural OH groups of montmorillonite. The bands correspond to bending vibrations of ALALOH and tridymite at 917 and 795 cm^{-1}, respectively. A complex band at 1039 cm^{-1} is related to the stretching vibrations of the Si–O groups. Water gave a broad band at 3429 cm^{-1} [24,25]. Bands at 523 and 470 cm^{-1} are due to the Al–O–Si and Si–O–Si bending vibrations, respectively. BCA samples reveal small changes in intensities of the transmission peaks due to the diminishing of some components related to kaolinite and the loss of water as a result of the sample heated up to 650 °C. No peaks have been observed related to CNTs as shown in spectrum C of Fig. 5.

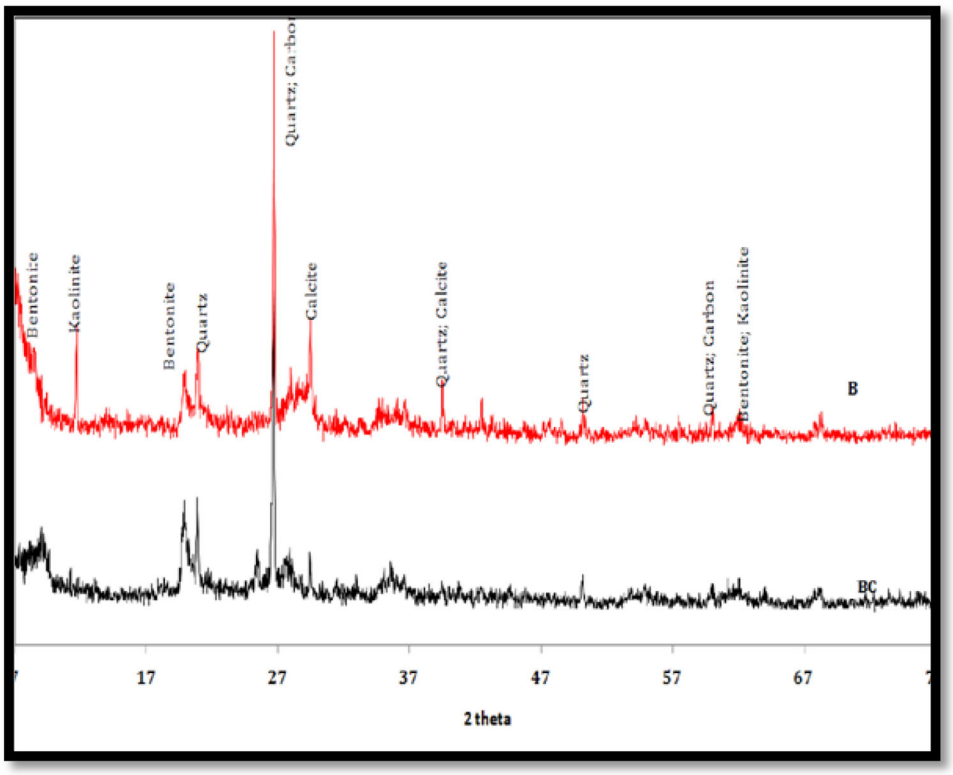

Fig. 4 XRD pattern of bentonite B and modified sample BCA

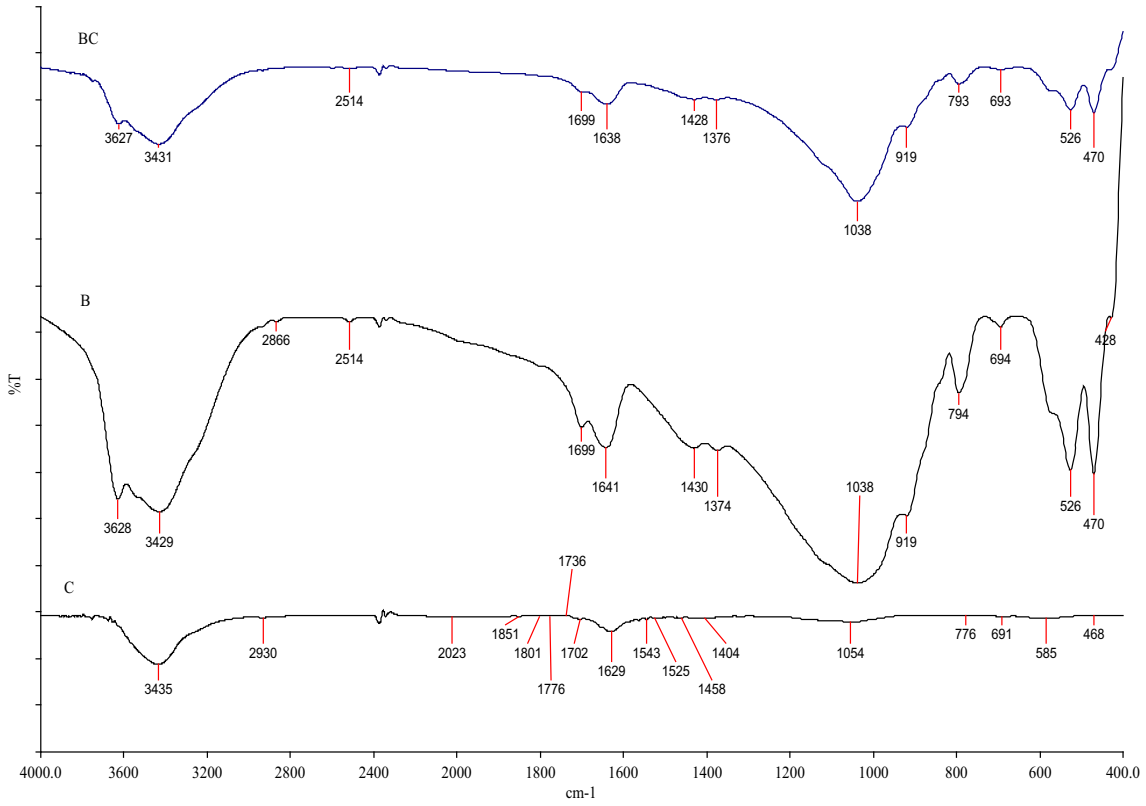

Fig. 5 FTIR spectra for carbon nanotube (C) and bentonite (B) nanocomposite (BCA)

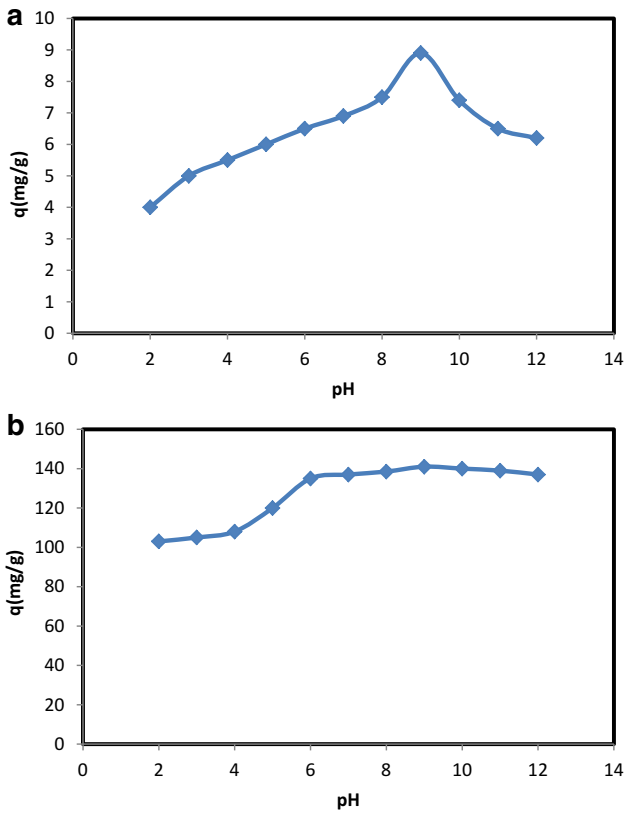

Fig. 6 **a** Effect of pH on the adsorption capacity of RhB on bentonite. **b** Effect of pH on the adsorption capacity of RhB on modified bentonite BCA

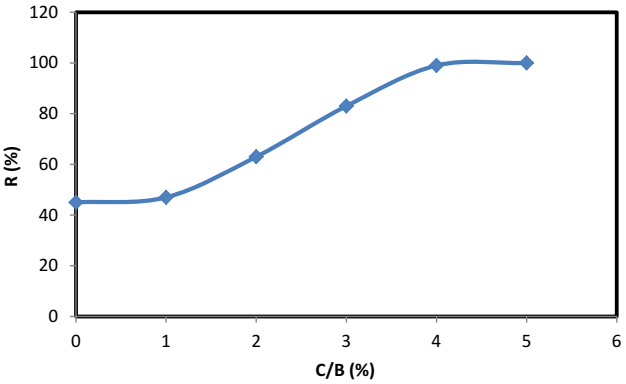

Fig. 7 Adsorption of RhB dye by different percentage of CNTs in bentonite

3.2 Adsorption of RhB Dye in Batch System

3.2.1 Effect of pH

The effect of pH on the adsorption of RhB on B and BCA was studied in different ranges between 2 and 12 as shown in Fig. 6a, b. The maximum removal for both samples was achieved at a pH of 9. The low adsorption of RhB dye by B and BCA at pH < 9 is due to the presence of excess positive ions that compete with the dye cationic group, and hence, a lower adsorption capacity of the dye is observed. However, the adsorption of RhB quickly decreased by BCA adsorbent at pH > 9. This can be attributed to the decrease of positive charge on the adsorbent surface, and the negatively charged site increases [25].

3.2.2 Optimization of CNT-to-B Ratio

In order to optimize the percentage of CNT in bentonite, the samples consisted of different CNT/B ratios (1, 2, 3, 4, 5 %) which were tested for removal of the RhB dye from an aqueous solution. One gram from each sample was combined with 100 mL of 100 mg/L dye solution in a 200-mL conical flask for 30 min using a magnetic stirrer. The pH of the solution was optimized at maximum adsorption (pH 9) and kept constant for all of the experiments. The result shows that the sample of bentonite with 5 % CNT gave a maximum removal of dye, as shown in Fig. 7. Therefore, the BCA sample with 5 % of CNT in bentonite has been identified as the best modifier. Its behavior in RhB dye adsorption and material structure will now be investigated during the following experimental part.

3.2.3 Effect of Contact Time

The effect of contact time on the adsorption capacity of RhB by the modified bentonite BCA is shown in Fig. 8. The adsorption is very fast initially and then slowly reaches the adsorption equilibrium in about 30 min. This can be attributed to large free surface sites available at an early stage of treatment time followed by less available sites due to repulsive forces between the dye and adsorbent phases [16]. Increase in adsorption capacity of BCA sample may be attributed to the fact that the CNTs of nanometers in size are dispersed among the silicate platelets on bentonite clay so that the high surface area of CNTs is available for the adsorption capacity and removal efficiency [28] as illustrated by SEM images in Fig. 3.

3.2.4 Effect of Adsorbent Dosage

The adsorption of the RhB dye onto BCA sample as a function of adsorbent dose (M) is shown in Fig. 9. The removal efficiency of RhB was increased with increasing sorbent amount until reaching (99.5 %) removal efficiency at 1.2 g (in 200 mL of 200 mg/L dye solution at pH 9) of BCA. The increase in removal efficiency with the BCA dosage can be attributed to the availability of large amounts of active sites of the adsorbent [29].

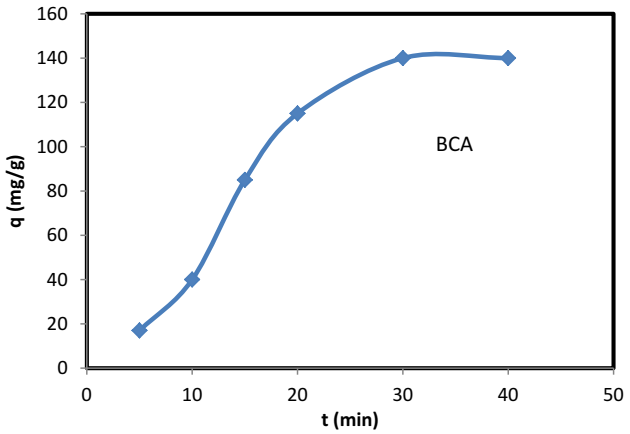

Fig. 8 Effect of contact time on adsorption capacity of RhB dye on BCA sample (pH 9, dosage of $B = 0.2$ g, $C_0 = 200$ ppm)

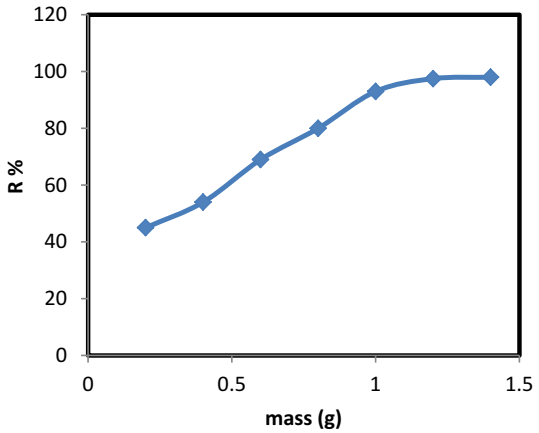

Fig. 9 Effect of BCA mass on removal efficiency of RhB dye ($C_0 = 200$ ppm, pH 9, contact time 30 min)

3.2.5 Effect of Initial Dye Concentration

The effect of initial red dye concentration on removal efficiencies of B and BCA is illustrated in Figs. 10 and 11, respectively. The removal efficiency decreases with increasing dye concentration from 25 to 200 mg/g for both results. The maximum removal at initial concentration of dye (25 mg/L) was found to be 52 % when B was used as an absorbent but decreased to 20 % at 200 mg/L of dye concentration. The maximum removal of the dye for the BCA sample was 96 % at 25 ppm dye concentration and decreased to 45 % at 200 ppm of dye concentration. The BCA sample reveals higher removal efficiency than B either with lower mass or with high concentration of dye used. Both behaviors are identical, which can be attributed to the increase in the ratio of the dye cations to the dosage of the adsorbent and the number of active adsorption sites required to accommodate the remaining adsorbent [26].

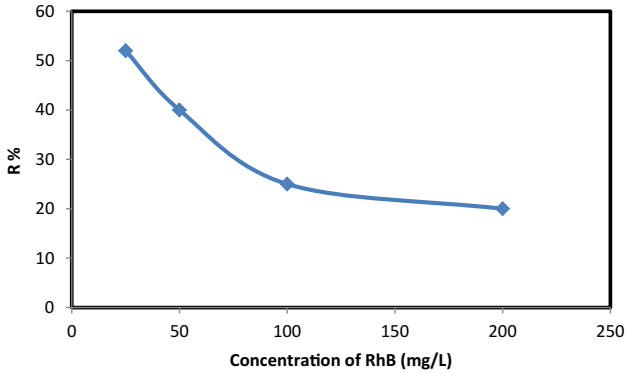

Fig. 10 Effect of initial dye concentration on removal efficiency (R %) of B sample (B dosage = 0.2 g, contact time = 30 min, pH 9)

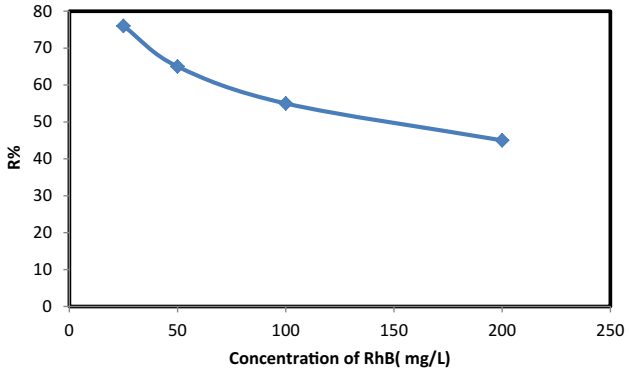

Fig. 11 Effect of initial dye concentration on removal efficiency (R %) of BCA sample (BCA dose = 0.2, contact time = 30 min, pH 9)

3.2.6 Adsorption Isotherms

The adsorption data for B and BCA were fitted into Langmuir and Freundlich isotherm equations. The linearization form of the Langmuir equation is as follows:

$$\frac{C_e}{q} = \frac{1}{(K_L q_m)} + \frac{C_e}{q_m} \tag{4}$$

where q, C_e, q_m and K_L are the amount of dye adsorbed at equilibrium (mg/g), concentration of adsorbate at equilibrium (mg/L), maximum adsorption capacity (mg/g) and Langmuir constant (L/mg), respectively. q_m and K_L constants were evaluated from the slope and intercept of the linear plots of C_e/q versus C_e, respectively, as shown in Fig. 12a for B and Fig. 12b for BCA.

The Langmuir maximum adsorption capacities for B and BCA were found to be 8.6 and 142.8 mg/g, respectively, and the maximum adsorption capacity of dye for the BCA adsorbent samples was about 14 times higher than that of B samples. It appears that the Langmuir model best fits the experimental results over the experimental range with good

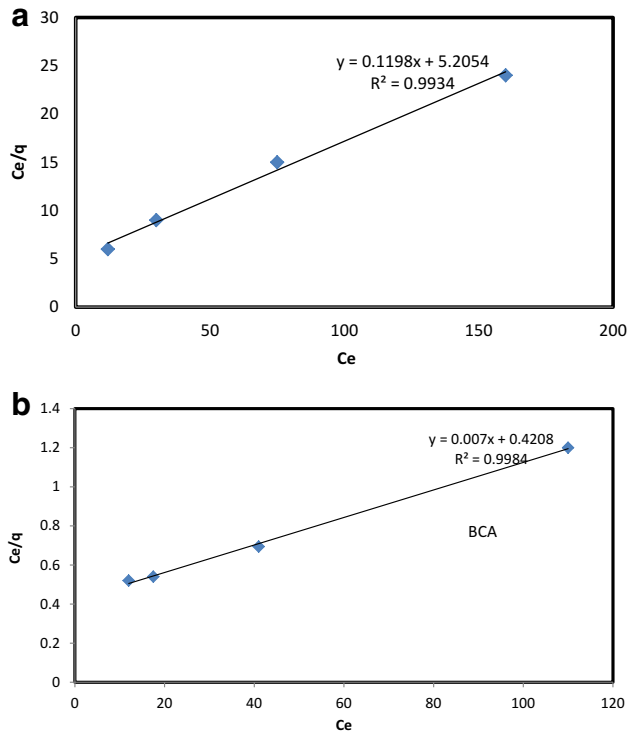

Fig. 12 **a** Langmuir isotherm plot for adsorption of RhB on B sample. **b** Langmuir isotherm plot for adsorption of RhB on BCA sample

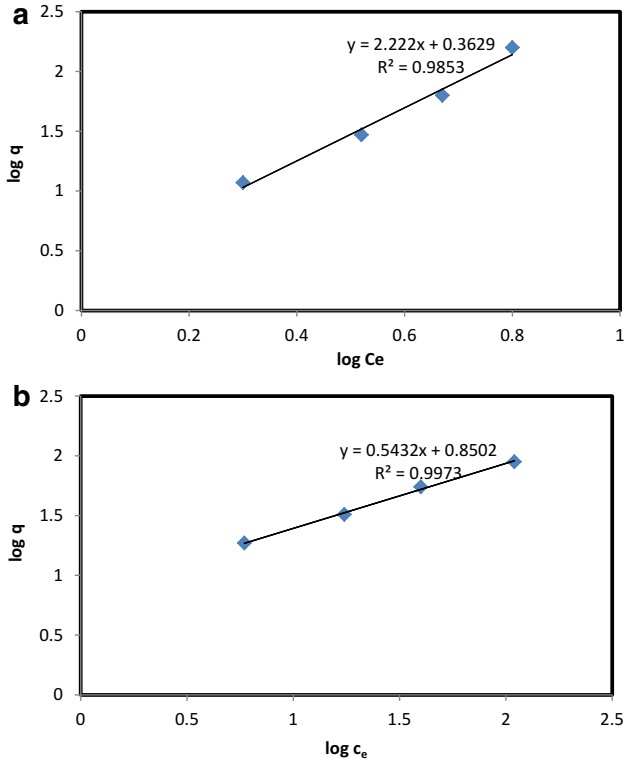

Fig. 13 **a** Freundlich isotherm plot for adsorption of RhB on B sample. **b** Freundlich isotherm plot for adsorption of RhB dye on BCA sample

Table 2 Isotherm parameters for RhB adsorbed onto BCA and B samples obtained by using Langmuir model

Sample	q_m	K_L	R^2
BCA	142.8	0.016	0.998
B	8.6	0.022	0.993

Table 3 Isotherm parameters for RhB adsorbed onto BCA and B samples obtained by using Freundlich model

Sample	K_F	n	R^2
BCA	7.07	1.841	0.997
B	2.3	0.450	0.985

Table 4 Comparison of adsorption capacity of some adsorbents for RhB removal

Adsorbents	Adsorption capacity (mg/g)	References
Bentonite	7.7	[31]
Carbon nanotubes	69	[32]
Malachite nanoparticles	23.47	[33]
Bentonite	8.6	This work
Modified bentonite BCA	142.8	This work

coefficients of correlation ($R^2 > 0.99$). The values of q_m, K_L and a linear correlation R^2 are given in Table 2.

Essential characteristics of the Langmuir isotherm can be expressed by a dimensionless constant called equilibrium parameter, RL, which is defined by the following equation [30]:

$$RL = 1/(1 + K_L C_0) \quad (5)$$

where C_0 is the initial dye concentration (mg/L). The nature of the adsorption process is either unfavorable (RL > 1), linear (RL = 1), favorable (0 < RL < 1) or irreversible (RL = 0).

Values of RL factor calculated for the sorption of the dye on modified bentonite (BCA) were found to be in the range of 0.38–0.741, indicating the favorable sorption.

The equilibrium adsorption data are also fitted to Freundlich's Eq. (6):

$$\log q = \log K_F + \frac{1}{n} \log C_e \quad (6)$$

where K_F and $1/n$ are Freundlich constants related to adsorption capacity and adsorption intensity, respectively, of the sorbent. The plot of $\log C_e$ versus $\log q$ in Fig. 13a for B and Fig. 13b for BCA is employed to evaluate the intercept K_F and the slope $1/n$. The values of K_F, n, and a linear correlation R^2 with Freundlich isotherms are given in Table 3. The best fit exhibited $R^2 = 0.937$ for B and $R^2 = 0.997$ for BCA.

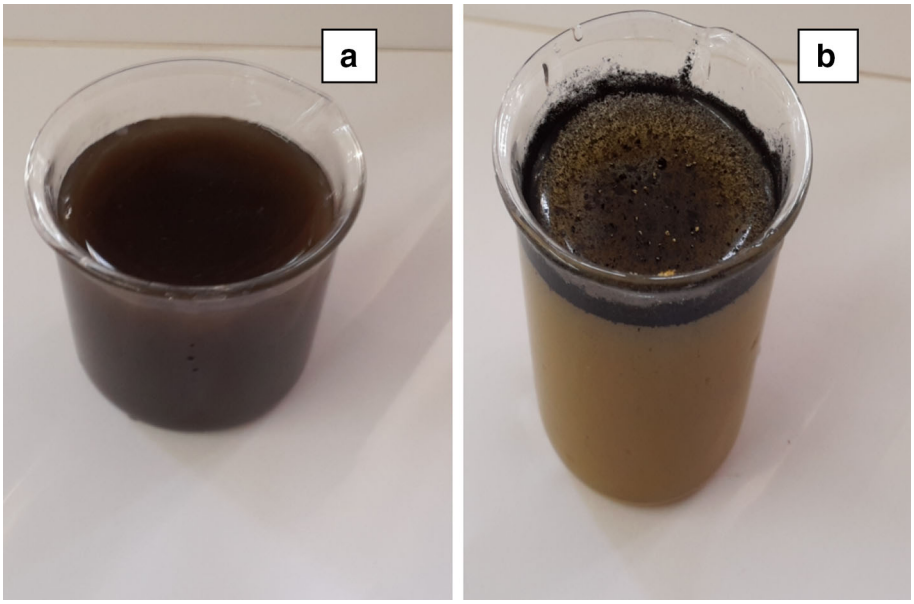

Fig. 14 Dispersibility behavior of **a** BCA nanocomposite sample, **b** none heated bentonite–CNTs mixture. Separation of CNTs from the mixture is clearly shown in figure (**b**)

The magnitude of n was 1.84 for the BCA sample and 0.450 for the B sample; accordingly, BCA has better favorable adsorption intensity (over the entire range of red dye concentration studied) than the adsorption intensity of B. The K_F value of the Freundlich equation (Table 3) also indicates that BCA has a higher adsorption capacity than the B samples. The adsorption capacities of the adsorbents for the removal of RhB have been compared with those of other adsorbents reported in literature, and the values of adsorption capacities are presented in Table 4. The values are reported in the form of monolayer adsorption capacity. The experimental data of the present investigation are comparable with the reported values [31–33]. The maximum adsorption capacity of RhB for the natural bentonite obtained by Dhankhar et al. [31] was 7.7 mg/g. This result agrees well with our work when only bentonite is used as an adsorbent for RhB removal from water. In another study, Mishra et al. [32] studied modified carbon nanotube, for RhB removal from aqueous solution. They reported that the carbon nanotube adsorbed RhB with the adsorption capability of ≈69 mg/g. Moreover, low adsorption capacity (23.47 mg/g) has been obtained when Malachite nanoparticle used as an adsorbent for removal of RhB from aqueous solution [33]. In this work, the adsorption capacity of the BCA increased to 142.8 mg/g. Compared with those obtained in the literature, the BCA is more effective for this purpose and surface properties of raw bentonite could be improved upon modification with CNTs.

Moreover, the heat-treated BCA nanocomposite powder shows better dispersibility in water compared with thermally untreated (bentonite–CNTs mixture) as shown in Fig. 14. This may be attributed to the formation of ceramic combination bonds within the composite structure of BCA sample after heat treatment of the sample at 650 °C. High dispersion property of BCA nanocomposite decreases the contact time due to the homogeneous immobilization within the water zone in batch experiment and can be easily removed from the system by sedimentation.

In order to estimate the feasibility of using such absorbent in purification of water in batch experimentally, one may look at this way: If we consider the worst cases of RhB concentration in water (200 mg/L), the amount of adsorbent (have adsorption capacity of 142.8 mg/g) needed to totally remove RhB dye from one metric cube batch of water would be 1.200 kg for totally saturated adsorbent. This would be in value about 60 USD based on commercial market material prices. Accordingly, the BCA can be considered cheaper compared with other costly nanomaterials.

4 Conclusions

Nanocomposite BCA was prepared, characterized and used as adsorbent for the removal of RhB from synthetic wastewater. It was found to have greater potential for the adsorption of RhB dye from aqueous solution in batch adsorption system. Batch experiment showed that the percentage of removal of RhB increases with the increase in the contact time, BCA dosage and pH and decreases with the increase in initial RhB concentration. The adsorption isotherms studies demonstrated that the adsorption processes can be well fitted by the Langmuir isotherm model with a higher correlation coefficient (0.990). This study has proved that a modified nanocomposite BCA was found to have a higher potential for the adsorption of RhB dye compared to the bentonite from an aqueous solution. In batch experiment, removal of RhB dye increased with increasing contact time (30 min of

contact time was found to be sufficient) and amount of BCA dose. It also decreased with increases in the amount of dye in the solution. The adsorption isotherms of dye were properly fitted to Langmuir and Freundlich models. The increase in adsorption capacity for the modified BCA sample was attributed mainly to the addition of CNTs and to dehydration of water during the heat treatment of the sample at high temperature as confirmed by SEM, XRD and FTIR observations. The resulting BCA sample shows high dispensability in water due to the good combination between CNTs and bentonite. These properties of BCA nanocomposite make them ideal for wastewater treatment technology. Besides, to develop some environment-friendly and cheap nanocomposite material is also the key work.

Acknowledgments The authors would like to thank the Department of Chemical Engineering in University of Sulyman Demirl/Turkey for their support.

References

1. Weber, E.J.; Adams, R.L.: Chemical- and sediment-mediated reduction of the azo dye disperse blue 79. Environ. Sci. Technol. **29**(5), 1163–1170 (1995)
2. Camargo, B.V.; Marales, M.A.: Azo dyes: characterization and toxicity—a review. Text. Light Ind. Sci. Technol. **2**(2) (2013)
3. Crini, G.: Non-conventional low cost adsorbents for dyes removal: a review. Bioresour. Technol. **97**(9), 1061–1085 (2006)
4. Rafatullah, M.; Sulaiman, O.; Hashim, R.; Ahmad, A.: Adsorption of methylene blue on low-cost adsorbents: a review. J. Hazard. Mater. **177**(1), 70–80 (2010)
5. Alsalhy, Q.F.; Albyati, T.M.; Zablouk, M.A.: A study of the effect of operating conditions on reverse osmosis membrane performance with and without air sparging technique. Chem. Eng. Commun. **200**(1), 1–19 (2013)
6. Chandra, T.C.; Mirna, M.M.; Sudaryanto, Y.; Ismadji, S.: Adsorption of basic dye onto activated carbon prepared from durian shell: studies of adsorption equilibrium and kinetics. Chem. Eng. J. **127**(1-3), 121–129 (2007)
7. Albayati, T.M.; Doyle, A.M.: Shape-selective adsorption of substituted aniline pollutants from wastewater. Adsorpt. Sci. Technol. **31**(5), 459–468 (2013)
8. Casal, B.; Merino, J.; Serratosa, J.M.; Ruiz-Hitzky, E.: Sepiolite-based materials for the photo- and thermal-stabilization of pesticides. Appl. Clay Sci. **18**(5–6), 245–254 (2001)
9. Iqbal, M.J.; Asiq, N.M.: Adsorption of dyes from aqueous solutions on activated charcoal. J. Hazard. Mater. **139**(1), 57–66 (2007)
10. Nasuha, N.; Zurainan, H.Z.; Maarof, H.I.; Zubir, N.A.; Amri, N.: Effect of cationic and anionic dye adsorption from aqueous solution by using chemically modified papaya seed. In: International Conference on Environment Science and Engineering, IPCBEE, vol. 8. Singapore (2011)
11. Neumann, M.G.; Gessner, F.; Schmitt, C.C.; Sartori, R.: Influence of the layer charge and clay particle size on the interactions between the cationic dye methylene blue and clays in an aqueous suspension. J. Colloid Interface Sci. **255**, 254–259 (2002)
12. Ayari, F.; Srasra, E.; Trabelsi-Ayadi, M.: Characterization of bentonitic clays and their use as adsorbent. Desalination **185**, 391–397 (2005)
13. El-Shishtawy, R.M.; Melegy, A.A.: Geochemistry and utilization of montmorillonitic soil for cationic dye removal. Adsorpt. Sci. Technol. **19**, 609–620 (2001)
14. Mandal, A.; Ojha, K.: Removal of colour from distillery wastewater by different processes. Indian Eng. **45**(4), 246–267 (2003)
15. Jin, X.; Jiang, M.; Shan, X.; Pei, Z.; Chen, Z.: Adsorption of methylene blue and orange II onto unmodified and surfactant-modified zeolite. J. Colloid Interface Sci. **328**(2), 243–247 (2008)
16. Mohammed, M.I.; Abdul Razak, A.A.; Hussein Al-Timimi, D.A.: Modified multiwalled carbon nanotubes for treatment of some organic dyes in wastewater. Adv. Mater. Sci. Eng. (2014). Article ID 201052. doi:10.1155/2014/201052
17. Selvam, P.P.; Preethi, S.; Basakaralingam, P.; Thinakaran, N.; Sivasamy, A.; Sivanesan, S.: Removal of rhodamine B from aqueous solution by adsorption onto sodium montmorillonite. J. Hazard. Mater. **155**, 39–44 (2008)
18. Madejova, J.: FTIR techniques in clay mineral studies. Vib. Spectrosc. **31**, 1–10 (2013)
19. Maksym, L.; Nikolai, L.; Eugene, V.: Hybrid multiwalled carbon nanotube-Laponite sorbent for removal of methylene blue from aqueous solutions. J. Colloid Interface Sci. **431**, 39–44 (2008)
20. Su, F.; Lu, C.: Adsorption kinetics, thermodynamics and desorption of natural dissolved organic matter by multiwalled carbon nanotubes. J. Environ. Sci. Health A **42**(11), 543–1552 (2007)
21. Shirmardi, M.; Mahvi, A.H.; Mesdaghinia, A.; Nasseri, S.; Nabizadeh, R.: Adsorption of acid red18 dye from aqueous solution using single-wall carbon nanotubes: kinetic and equilibrium. Desalin. Water Treat. **51**(34-36), 6507–6516 (2013)
22. Ting, S.; Shujuan, Z.; Tanju, K.: Adsorption of synthetic organic chemicals by carbon nanotubes: effects of background solution chemistry. Water Res. **44**, 2076–2074 (2010)
23. Peng, X.; Li, Y.; Luan, Z.; Di, Z.; Wang, H.; Tian, B.; Jia, Z.: Adsorption of 1,2-dichlorobenzene from water to carbon nanotubes. Chem. Phys. Lett. **376**(1-2), 154–158 (2003)
24. Lu, C.; Su, F.; Hu, S.: Surface modification of carbon nanotubes for enhancing BTEX adsorption from aqueous solutions. Appl. Surf. Sci. **254**(21), 7035–7041 (2008)
25. Baskaralingam, P.; Pulikesi, M.; Ramamurthi, V.; Sivanesan, S.: Equilibrium studies for the adsorption of acid dye onto modified hectorite. J. Hazard. Mater. B **136**, 989–992 (2006)
26. Sabri, A.A.; Albayati, T.M.; AlAzawı, R.A.: Synthesis of ordered mesoporous SBA-15 and its adsorption of methylene blue. Korean J. Chem. Eng. **32**(9), 1838–1841 (2015)
27. Önal, M.; Sarikaya, Y.: Thermal behaviour of a bentonite. J. Therm. Anal. Calorim. **90**, 167–172 (2007)
28. Jie, L.; Jiafen, P.: Removal of carbon tetrachloride from contaminated groundwater environment by adsorption method. In: Proceedings of the 4th International Conference on Bioinformatics and Biomedical Engineering (iCBBE), June 18–20, pp. 1–4. IEEE Xplore Press, Chengdu. doi:10.1109/ICBBE.2010.5517280 (2010)
29. Tang, R.; Lia, Q.; Cui, Y.; Zhang, H.Y.; Zhai, J.: Poly (aniline-co-aminophenol)/mesoporous silica SBA-15 composite. Polym. Adv. Technol. **22**(12), 2231–2236 (2011)
30. Ruthven, D.M.: Principles of Adsorption and Adsorption Processes. Wiley, New York (1985)

31. Dhankhar, R.; Hooda, A.: Fungal biosorption-an alternative to meet the challenges of heavy metal pollution in aqueous solutions. Environ. Technol. **32**, 467–491 (2011)
32. Mishra, A.K.; Arockiadoss, T.; Ramaprabhu, S.: Study of removal of azo dye by functionalized multi walled carbon nanotubes. Chem. Eng. **163**(3), 1026–1034 (2010). doi:10.1016/j.cej.2010.07.014
33. Zhu, H.Y.; Fu, Y.Q.; Jiang, R.; Jiang, J.H.; Xiao, L.; Zeng, G.M.; Zhao, S.L.; Wang, Y.: Adsorption removal of congo red onto magnetic cellulose/Fe_3O_4/activated carbon composite: Equilibrium, kinetic and thermodynamic studies. J. Chem. Eng. **173**, 494–502 (2011)